

Temperature-dependent x-ray fluorescent response from thermographic phosphors under x-ray excitation

Cite as: Appl. Phys. Lett. **119**, 034103 (2021); <https://doi.org/10.1063/5.0053469>

Submitted: 07 April 2021 . Accepted: 07 June 2021 . Published Online: 21 July 2021

 Eric R. Westphal, Alex D. Brown, Enrico C. Quintana, et al.



View Online



Export Citation



CrossMark

ARTICLES YOU MAY BE INTERESTED IN

[Influence of gallium surface saturation on GaN nanowire polytype selection during molecular-beam epitaxy](#)

Applied Physics Letters **119**, 031601 (2021); <https://doi.org/10.1063/5.0052659>

[Enhanced electrical transport through wrinkles in turbostratic graphene films](#)

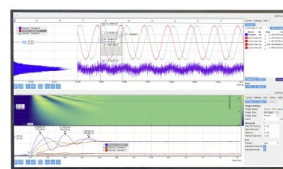
Applied Physics Letters **119**, 033102 (2021); <https://doi.org/10.1063/5.0056212>

[Control of antiferromagnetic resonance and the Morin temperature in cation doped \$\alpha\$ - \$\text{Fe}_{2-x}\text{M}_x\text{O}_3\$ \(M = Al, Ru, Rh, and In\)](#)

Applied Physics Letters **119**, 032408 (2021); <https://doi.org/10.1063/5.0053586>

Challenge us.

What are your needs for periodic signal detection?



Zurich Instruments



Temperature-dependent x-ray fluorescent response from thermographic phosphors under x-ray excitation

Cite as: Appl. Phys. Lett. **119**, 034103 (2021); doi: 10.1063/5.0053469

Submitted: 7 April 2021 · Accepted: 7 June 2021 ·

Published Online: 21 July 2021



View Online



Export Citation



CrossMark

Eric R. Westphal,^{1,a)} Alex D. Brown,¹ Enrico C. Quintana,² Alan L. Kastengren,³ Steven F. Son,¹ Terrence R. Meyer,¹ and Kathryn N. G. Hoffmeister^{2,a)}

AFFILIATIONS

¹School of Mechanical Engineering, Purdue University, West Lafayette, Indiana 47907, USA

²Sandia National Laboratories, Albuquerque, New Mexico 87123, USA

³X-ray Science Division, Advanced Photon Source, Argonne National Laboratory, Argonne, Illinois 60439, USA

^{a)}Authors to whom correspondence should be addressed: ewestph@purdue.edu and kngabet@sandia.gov

ABSTRACT

Phosphor thermometry has been successfully applied within several challenging environments. Typically, the thermographic phosphors are excited by an ultraviolet light source, and the temperature-dependent spectral or temporal response is measured. However, this is challenging or impossible in optically thick environments. In addition, emission from other sources (e.g., a flame) may interfere with the optical phosphor emission. A temperature dependent x-ray excitation/emission could alleviate these issues as x-rays could penetrate obscuring materials with no interference from flame luminosity. In addition, x-ray emission could allow for thermometry within solids while simultaneously x-ray imaging the structural evolution. In this study, select thermographic phosphors were excited via x-ray radiation, and their x-ray emission characteristics were measured at various temperatures. Several of the phosphors showed varying levels of temperature dependence with the strongest sensitivity occurring for YAG:Dy and ZnGa₂O₄:Mn. This approach opens a path for less intrusive temperature measurements, particularly in optically opaque multiphase and solid phase combustion environments.

Published under an exclusive license by AIP Publishing. <https://doi.org/10.1063/5.0053469>

Conventional phosphor thermometry is a temperature sensing technique involving the excitation of thermographic phosphor particles via a light source in the ultraviolet (UV) or near UV range.^{1–5} When excited, the phosphors undergo electronic energy level transitions to higher energy states, followed by relaxation back to the ground state causing the emission of photons that are redshifted from the excitation source. Depending on the phosphor temperature, the emission spectrum can broaden or shift in wavelength or intensity. The characterization of phosphor emission for temperature sensitivity can fall into two categories. The first involves time-resolved measurements of the photoemission in which the lifetime decay,^{2,3,6} rise time,^{7,8} or phase shift of the emission from an oscillating excitation source^{2,3,9} varies with temperature and is measured. The second category involves time-integrated methods, which typically involve measuring two different spectral bands of a phosphor's emission to create a two-color ratio calibration for temperature.^{2,3,10,11}

Conventional phosphor thermometry has been employed to measure temperature within combustion and heated environments,

such as diesel engines,^{12–14} gas turbines,^{15–18} and gaseous flows.^{19–22} However, traditional excitation and emission schemes fail in optically thick gaseous flow conditions and cannot be applied within reacting opaque solids. An alternative approach is needed for non-intrusive measurements.

X rays are sufficiently energetic to pass through many solid materials and optical absorbers that inhibit UV or near-UV excitation. While UV photon excitation causes energy level transitions within the valence band of the phosphor particles, incident x-ray radiation has sufficient energy to penetrate further into the atoms composing the phosphors, interacting with inner shell electrons. This can cause x-ray fluorescence (XRF), which gives rise to x-ray emission spectroscopy (XES), a technique in which inner shell electrons are ejected from the atoms due to the incident x-rays.^{23,24} An outer-shell electron then fills this vacancy, producing an x-ray photon during the transition. The energies of x-rays produced in this manner are characteristic to the element of the atom being excited.

As x-ray excitation penetrates deep into the core of atoms, the characteristic x-ray emission produced is typically considered to be

independent of temperature. This approximation can break down in crystalline structures containing transition metals and rare-earth elements, particularly those in which core holes left by the x-ray excitation couple strongly with valence electrons.²⁵ Since the core hole is coupled with valence electrons, final energy states available to electrons filling the hole are dependent on the location of the valence electron shell positions, leading to temperature dependence as seen in Fig. 1. In these complex systems, spin pairing, material structure, insulator-metal transitions, magnetic transitions, and electronic screening lead to temperature- and pressure-dependent transitions that affect the structure of the characteristic x-ray lines.^{26–31}

In the case of d-electron materials (those containing elements with unfilled d-shells such as Y, Ce, and Mn), particularly oxides, the average electron distance is much greater than the Bohr radius, creating strong electron–electron repulsion.³⁰ D-shells have internal degrees of freedom, which, when coupled into a lattice structure, can lead to strong movement coupling effects between electrons in materials, a phenomenon known as electron correlation. Where electron correlation is high, electronic transitions, including those involved in x-ray spectroscopy, have high susceptibility to temperature, pressure, magnetic fields, and doping effects. In these d-electron materials, the K_{β} ($3p \rightarrow 1s$) and K_{α} ($2p \rightarrow 1s$) transitions are shown to be sensitive to the transition-metal spin state.^{26–30} See Ref. 29 for a detailed description of the multiplet spin structure. F-electron systems, materials with partially filled 4f and 5f shells such as Dy and Eu, have also shown strong electron correlation.^{29,30}

If phosphor XRF is thermographic, similar to visible emission, temperature measurements of a sample could be made within an opaque boundary—e.g., oven walls, sooty flames, or solid rocket propellant. The limiting factor would become collection of the x-rays produced by the phosphors, which could have sufficient energy to pass through many materials. In addition, x-ray excitation would allow for simultaneous temperature measurement and x-ray imaging of the material structure. However, while the pressure effects and material/chemical transitions have been well characterized in UV and visible emission bands,³² further investigation is needed in the x-ray regime. The objective of this work is to determine the temperature sensitivity of several select thermographic phosphors during x-ray excitation/emission at atmospheric pressures.

While the focus of the present study is the characterization of phosphor XRF for temperature sensitivity, scintillation will occur

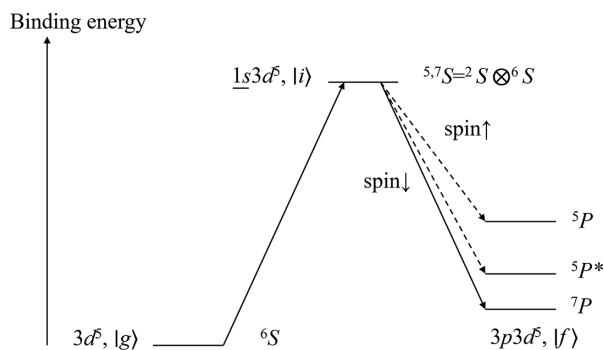


FIG. 1. K_{β} process ($3p \rightarrow 1s$) in the case of a $3d^5$ ion. Reprinted with permission from Rueff and Shukla, Rev. Mod. Phys. **82**, 864 (2010). Copyright 2010 American Physical Society.²⁹

simultaneously; visible photons will be produced by the phosphors. This visible emission can be categorized as a form of x-ray excited optical luminescence (XEOL). A separate manuscript by the authors describes the thermography of this XEOL captured simultaneously with the results presented in this study, and readers are referred to this manuscript for a detailed description of the temperature sensitivity of the visible emission from the phosphors.³³

Phosphors selected for testing were chosen based on the desired applications and XEOL produced. Of the phosphors used in this study, $Y_3Al_5O_{12}:Dy$ or YAG:Dy (PTL QMK66), $BaMgAl_{10}O_{17}:Eu$ or BAM (PTL KEMK63), $La_2O_2S:Eu$ (PTL SKL63), $Mg_3F_2GeO_4:Mn$ (PTL EQD25), $ZnGa_2O_4:Mn$ (PTL GPK25), and ZnO (Just Pigments, ZN001–1) were selected based on their usefulness to combustion applications.^{19,34–36} In addition, the phosphors $Gd_2O_2S:Tb$ (PTL UKL65) and $Y_2SiO_5:Ce$ (PTL QBK58) were selected for their usefulness as x-ray scintillators, materials used in x-ray detectors that convert incident x-ray photons to visible light.^{37–39} The results for BAM, $La_2O_2S:Eu$, $Mg_3F_2GeO_4:Mn$, $Gd_2O_2S:Tb$, and $Y_2SiO_5:Ce$ are included in the supplementary material.

Phosphors were tested independently with each sample prepared by mixing the phosphor powder with ethanol. A brush was then used to coat the mixture onto an aluminum substrate and allowed to dry. Aluminum was selected due to the low energies of its characteristic x-ray emission lines (<2 keV). This avoids interference between potentially thermographic emission lines originating from the transition metals and rare-earth elements (typically >5 keV in the materials tested) in the phosphors and the substrate.

Once prepared, phosphor samples were then placed on a hot plate alongside a blank aluminum substrate, as shown in Fig. 2. This blank substrate was used for collecting background energy spectra that were subtracted later during data post processing. A thermocouple was placed on the surface of the hot plate between the coated and blank aluminum substrates to monitor the sample's temperature as each was heated and cooled.

This setup was placed in the x-ray beam path of beamline 7-BM-B at the Advanced Photon Source (APS) at Argonne National Laboratory.

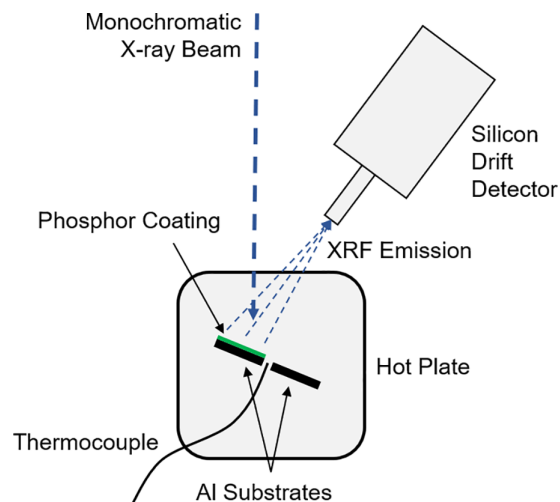


FIG. 2. Setup for x-ray excitation and emission detection at the Advanced Photon Source.

This beamline was set to monochromatic beam mode during phosphor excitation, producing x-rays at 67.6 keV with a 1% bandpass. The monochromatic beam mode was chosen to reduce the effects of the beam energy profile on the measurements. A silicon drift x-ray detector (Hitachi Vortex, 490 μm thick) was used to capture the energy spectra of the x-ray fluorescence produced by each phosphor and substrate. The incident x-rays were attenuated with various combinations of Si, Cu, and Ge filters to optimize the intensity of the x-ray signal detected for each phosphor and to test whether the incident flux changed the shape of the detected XRF emission. During testing, background and phosphor signal spectra were captured at each temperature and for each phosphor. A total of ten background spectra and 50 phosphor signal spectra were obtained at each temperature for signal averaging. All spectra presented in the results of this study were averaged and background subtracted. The hot plate was placed on a computer-controlled translation stage, which allowed the signals to be captured at the same locations.

YAG:Dy was tested at temperatures ranging from room temperature up to 333 $^{\circ}\text{C}$, and the average x-ray emission spectra captured in this range are seen in Fig. 3. The peaks seen in Fig. 3(a) are labeled with their corresponding emission lines. Similar labels are used throughout this paper for each phosphor tested and their resulting emission lines. Note that lines labeled with the subscript α are made up of the α_1 and α_2 lines of the corresponding transition group (K series, L series, etc.) of a given element. Emission lines such as these that cannot be resolved individually by the x-ray detector are grouped together in this way throughout this paper. Likewise, lines labeled with the subscript β consist of the many β lines of the corresponding transition group of a given element, which are in close proximity to one another.

The spectra shown in Fig. 3(a) are normalized to the Dy L_{α} line at each temperature centered at about 6.5 keV. The normalization value for each temperature was obtained by performing a trapezoidal integration under the selected peak. This method of normalization is used throughout this work. The shaded regions seen in the inset of Fig. 3(a) (and throughout these results) represent the standard deviation of the average spectrum calculated for each temperature. The Y K_{α} line can clearly be seen to shift in intensity with temperature, whereas the two Dy L series lines remain relatively constant over the temperature range. Small overlaps can be seen between some of the standard deviations of the average spectra of the Y K_{α} line; however, the general trend of shifting intensity with changes in temperature is still apparent in the data. In addition, small shifts with temperature can be discerned in the Y K_{β} line, which is highlighted along with the temperature sensitivity of the Y K_{α} line in the intensity ratios shown in Fig. 3(b). The integrated area under each of these lines was calculated again using a trapezoidal integration method. These values were used in the numerator of the ratio calculation, and the corresponding integrated areas under the Dy L_{α} line were used in the denominator. Sensitivity to temperature is apparent for each ratio calibration calculated using the selected lines, although significant overlap can be seen between the standard deviations of the ratios calculated at each temperature.

Results for $\text{ZnGa}_2\text{O}_4\text{:Mn}$ normalized to the Ga K_{β} emission line are seen in Fig. 4. This phosphor differs from YAG:Dy in that it is doped with a transition metal rather than a rare-earth element, though the partially-filled d-shell of Mn suggests that the physics leading to

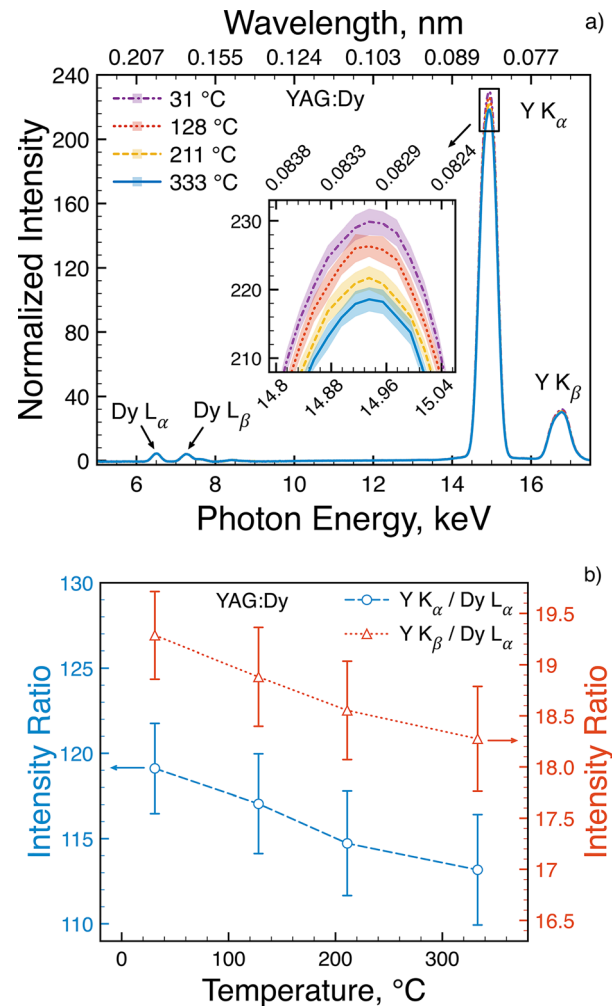


FIG. 3. (a) The average x-ray emission spectra of YAG:Dy at various temperatures normalized to the Dy L_{α} line. Shaded regions represent standard deviation of each average spectrum. (b) Intensity ratio calibrations calculated using the Y K_{α} and Y K_{β} lines (numerators) and the Dy L_{α} line (denominator).

temperature-dependence should be similar. Mn lines were not sufficiently separated from other emission lines to be usable and, thus, are not shown in the figure. Both the Ga and Zn K_{α} lines exhibit some degree of temperature sensitivity with this normalization. The standard deviation of the average spectra seen in the inset of Fig. 4(a) highlights this temperature sensitivity of the Ga K_{α} line. To further quantify the thermographic potential of this phosphor's x-ray emission, an intensity ratio calibration is shown in Fig. 4(b) between the Ga K_{α} line and the Ga K_{β} line, calculated using each spectrum collected at each temperature tested. Like the results for YAG:Dy, large standard deviations are apparent in the calculated ratios, although a general trend with temperature is present. These results are limited by the low number of temperature data points collected for this phosphor, which was due to time constraints at the beamline. More data points will be needed in the future to further characterize this phosphor's emission.

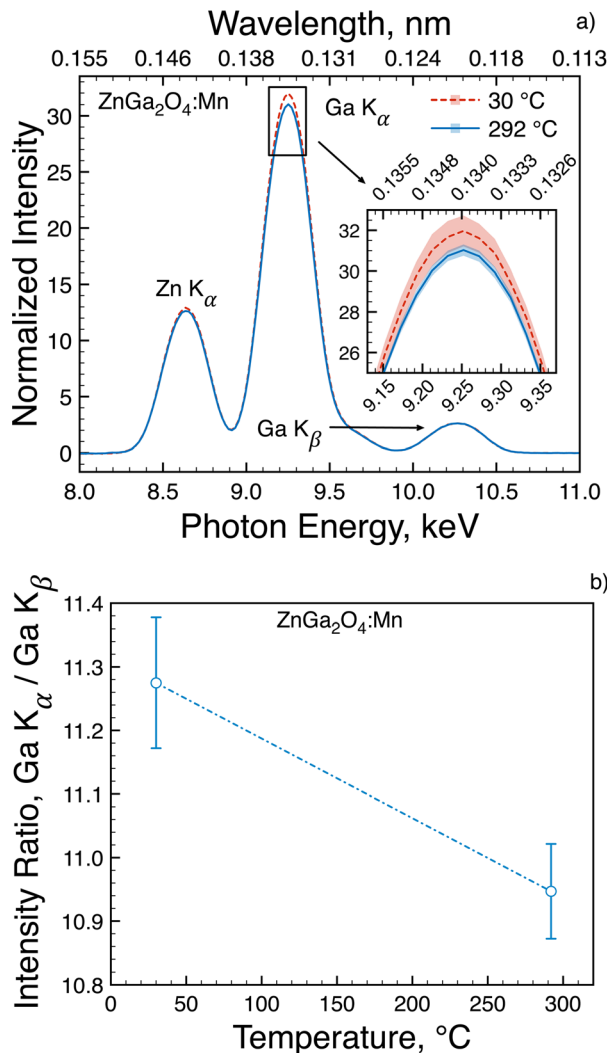


FIG. 4. (a) The average x-ray emission spectra of $\text{ZnGa}_2\text{O}_4:\text{Mn}$ at various temperatures normalized to the Ga K_β line. Shaded regions represent standard deviation of each average spectrum. (b) An intensity ratio calibration calculated using the Ga K_α line (numerator) and the Ga K_β line (denominator).

Though undoped, pure ZnO is known to produce a thermographic optical emission.³⁶ However, Zn does not have the properties (unfilled d- or f-shells) that would suggest thermographic response in the x-ray spectrum. The non-normalized energy spectra obtained for this phosphor are shown in Fig. 5, along with spectra normalized to the Zn K_β line (in the inset). No temperature dependence is seen in the data when normalized, though significant changes in intensity are seen in the non-normalized data. Note that two average spectra at 30 °C are shown. These two spectra differ in the time they were captured. One was collected before any heating of the sample had occurred (BH), and the other was captured after the sample had been heated to its maximum temperature of 282 °C and then allowed to cool back down to 30 °C (AC). The significant hysteresis in the data suggests that ZnO may have undergone a chemical transition similar

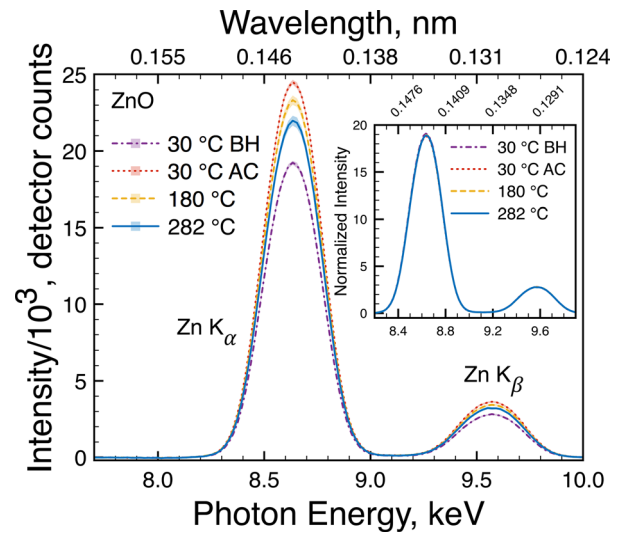


FIG. 5. The average x-ray emission spectra of ZnO at various temperatures. The normalized (inset) and non-normalized data showing the spectra at each temperature, including two sets of data obtained at 30 °C, one before the sample was subjected to any heating (BH) and another after the sample was heated to the maximum temperature of 282 °C and allowed to cool back down to 30 °C (AC). Spectra in the inset were normalized to the Zn K_β line. Shaded areas in the main plot represent standard deviation of each average spectrum.

to that seen in LaCoO_3 in Ref. 27. Nonetheless, this potential hysteresis does not appear to affect the relative temperature dependence of the two lines, which show very close equivalence and illustrate the precision of the measurements.

It was found that the best candidates for temperature sensing using x-ray excitation/emission within the temperature ranges studied are YAG:Dy and $\text{ZnGa}_2\text{O}_4:\text{Mn}$ for the configuration/materials considered; both exhibit clear temperature sensitivity in their XRF responses. Alternatively, it may be possible to utilize multiple phosphors with and without temperature sensitivity in combination to achieve the same result. Other materials, particularly those with constituents whose K series emission lines were beyond our detection limits, may also be viable options. These K series emission lines would be particularly useful for scenarios with significant optical access challenges, as the harder x-rays will better penetrate the optical obstruction.

The results described here are consistent with the hypothesis that complex spin-state multiplet structures are responsible for temperature-dependence in the x-ray region.²⁹ Supporting this hypothesis is the lack of temperature response in ZnO, as it is the only material tested that does not have a matrix containing elements with partially filled d- or f-shells. This suggests that while many of the known optically thermographic materials meet the requirements for x-ray temperature dependence (complex crystal matrices with elements containing partially filled d- or f-shells, particularly those in oxide form or dopants), researchers should not limit themselves to these materials. Another key consideration is that due to the strong pressure-dependence of this mechanism, future research in the x-ray spectrum must take pressure into account when determining the viability of these materials.

Temperature ranges tested in this study were selected in part based on the ranges of sensitivity of the visible response from these

phosphors. However, based on the results for $\text{Gd}_2\text{O}_2\text{S:Tb}$ (see the [supplementary material](#)), this may not be a good indication for the sensitivity of the x-ray response, as the x-ray emission of this phosphor showed no temperature sensitivity over this range. However, there may be temperature-sensitive emissions at higher x-ray energies beyond the range of the detector used in this study.

The upper limit of $\sim 300^\circ\text{C}$ seen throughout this work was dictated by the hot plate selected as the heating source for these experiments. Future work will employ a higher temperature and more controlled heating source to explore higher temperature ranges. In addition, the low number of temperature data points seen in these results was due to time constraints at the beamline. Finer temperature increments over an extended time frame will need to be considered in future work at the beamline.

All measurements in this paper were collected with a monochromatic beam at APS. An important consideration for measurements using lab-scale or medical x-ray sources will be the spectrum of the incident photons. A broadband spectrum that includes energies of the XRF emission lines studied will need to be convolved in order to make the technique independent of the excitation source.

In summary, the x-ray energy spectra of several thermographic phosphors were measured at various temperatures during x-ray excitation and found to have temperature sensitivity. Based on these initial results for select phosphors, the two primary candidates for future characteristic x-ray based temperature sensing measurements are YAG:Dy and $\text{ZnGa}_2\text{O}_4\text{:Mn}$. The results were consistent with changes in the x-ray emission spectrum being dependent upon the multiplet structure, as described in previous studies.^{26–30} In particular, the results indicate that additional phosphors (and non-phosphor materials) containing metals with partially filled d- or f-shells should be tested in the future, as this property suggests that they may exhibit the spin state splitting characteristic of this type of complex multiplet structure. Extended temperature ranges should also be investigated in the future for all the phosphors tested here to determine if their sensitivity lies in or extends beyond the regions in this study.

See the [supplementary material](#) for the x-ray fluorescence results obtained for the phosphors BAM , $\text{La}_2\text{O}_2\text{S:Eu}$, $\text{Mg}_3\text{F}_2\text{GeO}_4\text{:Mn}$, $\text{Gd}_2\text{O}_2\text{S:Tb}$, and $\text{Y}_2\text{SiO}_5\text{:Ce}$.

The authors would like to thank Walt Gill for input into developing the research topics explored in this work. The authors would also like to thank the Office of Naval Research as this research is funded, in part, through project Award No. N00014-16-1-2557 and by the Air Force Office of Scientific Research through Award No. FA9550-15-1-0102 to Purdue University. Support was also provided by NASA Space Technology Research Fellowship No. 80NSSC17K0190. This research used resources of the Advanced Photon Source, a U.S. Department of Energy (DOE) Office of Science User Facility operated for the DOE Office of Science by Argonne National Laboratory under Contract No. DE-AC02-06CH11357. Sandia National Laboratories is a multimission laboratory managed and operated by National Technology and Engineering Solutions of Sandia, LLC, a wholly owned subsidiary of NTESS, for the U.S. Department of Energy's National Nuclear Security Administration under Contract No. DE-NA0003525. SAND2021-7342 J.

DATA AVAILABILITY

The data that support the findings of this study are available from the corresponding authors upon reasonable request.

REFERENCES

- A. D. Casey, Z. A. Roberts, A. Satija, R. P. Lucht, T. R. Meyer, and S. F. Son, "Dynamic imaging of the temperature field within an energetic composite using phosphor thermography," *Appl. Opt.* **58**, 4320–4325 (2019).
- J. Brübach, C. Pflitsch, A. Dreizler, and B. Atakan, "On surface temperature measurements with thermographic phosphors: A review," *Prog. Energy Combust. Sci.* **39**, 37–60 (2013).
- M. Aldén, A. Omrane, M. Richter, and G. Särner, "Thermographic phosphors for thermometry: A survey of combustion applications," *Prog. Energy Combust. Sci.* **37**, 422–461 (2011).
- G. Särner, M. Richter, and M. Aldén, "Investigations of blue emitting phosphors for thermometry," *Meas. Sci. Technol.* **19**, 125304 (2008).
- A. H. Khalid and K. Kontis, "Thermographic phosphors for high temperature measurements: Principles, current state of the art and recent applications," *Sensors* **8**, 5673–5744 (2008).
- A. Omrane, F. Ossler, and M. Aldén, "Two-dimensional surface temperature measurements of burning materials," *Proc. Combust. Inst.* **29**, 2653–2659 (2002).
- A. H. Khalid and K. Kontis, "2D surface thermal imaging using rise-time analysis from laser-induced luminescence phosphor thermometry," *Meas. Sci. Technol.* **20**, 025305 (2009).
- T. Cai, Y. Park, S. Mohammadshahi, and K. C. Kim, "Rise time-based phosphor thermometry using $\text{Mg}_4\text{FGeO}_6\text{:Mn}_4$," *Meas. Sci. Technol.* **32**, 015201 (2021).
- S. W. Allison, D. L. Beshears, M. R. Cates, M. Paranthaman, and G. T. Gilles, "LED-induced fluorescence diagnostics for turbine and combustion engine thermometry," *Opt. Diagnostics Fluids, Solids, Combust.* **4448**, 28–35 (2001).
- L. P. Goss, A. A. Smith, and M. E. Post, "Surface thermometry by laser-induced fluorescence," *Rev. Sci. Instrum.* **60**, 3702–3706 (1989).
- A. L. Heyes, S. Seefeldt, and J. P. Feist, "Two-colour phosphor thermometry for surface temperature measurement," *Opt. Laser Technol.* **38**, 257–265 (2006).
- T. Husberg, S. Gjirja, I. Denbratt, A. Omrane, M. Aldén, and J. Engström, "Piston temperature measurement by use of thermographic phosphors and thermocouples in a heavy-duty diesel engine run under partly premixed conditions," in SAE Technical Paper (2005).
- J. T. Kashdan, B. Thirouard, S. Sae, I. Journal, J. T. Kashdan, and B. Thirouard, "A comparison of combustion and emissions behaviour in optical and metal single-cylinder diesel engines," *SAE Int. J. Engines* **2**, 1857–1872 (2009).
- T. Aizawa and H. Kosaka, "Laser-induced phosphorescence thermography of combustion chamber wall of diesel engine," *SAE Int. J. Fuels Lubr.* **1**, 549–558 (2008).
- K. W. Tobin, S. W. Allison, M. R. Gates, G. J. Capps, D. L. Beshears, M. Cyr, and B. W. Noel, "High-temperature phosphor thermometry of rotating turbine blades," *AIAA J.* **28**, 1485–1490 (1990).
- P. Nau, Z. Yin, O. Lammel, and W. Meier, "Wall temperature measurements in gas turbine combustors with thermographic phosphors," *J. Eng. Gas Turbines Power* **141**, 041021 (2019).
- J. P. Feist, A. L. Heyes, and S. Seefeldt, "Thermographic phosphor thermometry for film cooling studies in gas turbine combustors," *Proc. Inst. Mech. Eng. Part A* **217**, 193–200 (2003).
- J. P. Feist, A. L. Heyes, and S. Seefeldt, "Thermographic phosphors for gas turbines: instrumentation development and measurement uncertainties," in 11th International Symposium on Application of Laser Technique to Fluid Mechanics (2002).
- M. Lawrence, H. Zhao, and L. Ganippa, "Gas phase thermometry of hot turbulent jets using laser induced phosphorescence," *Opt. Express* **21**, 12260–12281 (2013).
- J. P. J. Van Lipzig, M. Yu, N. J. Dam, C. C. M. Luijten, and L. P. H. De Goey, "Gas-phase thermometry in a high-pressure cell using $\text{BaMgAl}_{10}\text{O}_{17}\text{:Eu}$ as a thermographic phosphor," *Appl. Phys. B* **111**, 469–481 (2013).
- A. Omrane, P. Petersson, M. Aldén, and M. A. Linne, "Simultaneous 2D flow velocity and gas temperature measurements using thermographic phosphors," *Appl. Phys. B* **92**, 99–102 (2008).

- ²²B. Fond, C. Abram, A. L. Heyes, A. M. Kempf, and F. Beyrau, "Simultaneous temperature, mixture fraction and velocity imaging in turbulent flows using thermographic phosphor tracer particles," *Opt. Express* **20**, 22118–22133 (2012).
- ²³P. J. Potts and P. C. Webb, "X-ray fluorescence spectrometry," *J. Geochem. Explor.* **44**, 251–296 (1992).
- ²⁴R. Jenkins, *X-Ray Fluorescence Spectrometry*, 2nd ed. (Wiley-Interscience, New York, 1999).
- ²⁵F. de Groot and A. Kotani, *Core Level Spectroscopy of Solids* (CRC Press, Boca Raton, FL, 2008).
- ²⁶G. Vankó, T. Neisius, G. Molnár, F. Renz, S. Kárpáti, A. Shukla, and F. M. F. De Groot, "Probing the 3D spin momentum with x-ray emission spectroscopy: The case of molecular-spin transitions," *J. Phys. Chem. B* **110**, 11647–11653 (2006).
- ²⁷G. Vankó, J.-P. Rueff, A. Mattila, Z. Németh, and A. Shukla, "Temperature- and pressure-induced spin-state transitions in LaCoO₃," *Phys. Rev. B* **73**, 24424 (2006).
- ²⁸D. P. Kozlenko, N. O. Golosova, Z. Jiráček, L. S. Dubrovinsky, B. N. Savenko, M. G. Tucker, Y. L. Godec, and V. P. Glazkov, "Temperature- and pressure-driven spin-state transitions in LaCoO₃," *Phys. Rev. B* **75**, 64422 (2007).
- ²⁹J. P. Rueff and A. Shukla, "Inelastic x-ray scattering by electronic excitations under high pressure," *Rev. Mod. Phys.* **82**, 847–896 (2010).
- ³⁰H. K. Mao, X. J. Chen, Y. Ding, B. Li, and L. Wang, "Solids, liquids, and gases under high pressure," *Rev. Mod. Phys.* **90**, 15007 (2018).
- ³¹A. Mattila, T. Pylkkänen, J. P. Rueff, S. Huotari, G. Vankó, M. Hanfland, M. Lehtinen, and K. Hämäläinen, "Pressure induced magnetic transition in siderite FeCO₃ studied by x-ray emission spectroscopy," *J. Phys. Condens. Matter.* **19**, 386206 (2007).
- ³²J. Brübach, A. Dreizler, and J. Janicka, "Gas compositional and pressure effects on thermographic phosphor thermometry," *Meas. Sci. Technol.* **18**, 764–770 (2007).
- ³³E. R. Westphal, A. D. Brown, E. C. Quintana, A. L. Kastengren, S. F. Son, T. R. Meyer, and K. N. G. Hoffmeister, "Visible emission spectra of thermographic phosphors under x-ray excitation," *Meas. Sci. Technol.* **32**, 094008 (2021).
- ³⁴M. R. Cates, K. W. Tobin, and D. Barton Smith, "Evaluation of thermographic phosphor technology for aerodynamic model testing," Technical Report No. ORNL/ATD-40ON: DE91005631 (Oak Ridge National Lab., TN, 1990).
- ³⁵S. Allison, M. Cates, and D. Beshears, "A survey of thermally sensitive phosphors for pressure sensitive paint applications," in *Proceedings of the International Instrumentation Symposium* (IAEA, 2000), pp. 29–38.
- ³⁶C. Abram, B. Fond, and F. Beyrau, "High-precision flow temperature imaging using ZnO thermographic phosphor tracer particles," *Opt. Express* **23**, 19453–19468 (2015).
- ³⁷M. Nikl, "Scintillation detectors for x-rays," *Meas. Sci. Technol.* **17**, R37–R54 (2006).
- ³⁸C. W. E. Van Eijk, "Inorganic scintillators for medical imaging," *Phys. Med. Biol.* **47**, R85–R106 (2002).
- ³⁹P. A. Rodnyi, *Physical Processes in Inorganic Scintillators* (CRC Press, Boca Raton, FL, 1997).